Geophys. J. Int. (2007) **169,** 421–434 doi: 10.1111/j.1365-246X.2007.03305.x

A study of spectral methods of estimating the depth to the bottom of magnetic sources from near-surface magnetic anomaly data

D. Ravat,[1] A. Pignatelli,[2] I. Nicolosi[2] and M. Chiappini[2]

[1]*Department of Geology, Southern Illinois University Carbondale, Carbondale,* IL 62901-4324, *USA. E-mail: ravat@geo.siu.edu*
[2]*Istituto Nazionale di Geofisica e Vulcanologia, Via di Vigna Murata* 605, 00143 *Roma, Italy*

Accepted 2006 November 16. Received 2006 November 1; in original form 2006 June 15

SUMMARY

Based on a critical evaluation of several different spectral magnetic depth determination techniques on areally large synthetic layered and random magnetization models, we recommend the following considerations in the usage of the methods as necessary prerequisites to successful bottom depth determinations: (1) using windows with sufficient width to ascertain that the response of the deepest magnetic layer is captured and by verifying the spectra and computing the depth estimates with the largest possible windows (>300–500 km); (2) avoiding filtering to remove arbitrary regional fields, accomplished by compiling magnetic anomalies derived from modern spherical harmonic degree 13 Earth's main field models [e.g. recent International Geomagnetic Reference Field models (IGRF) or Comprehensive models (CM)]; (3) ascertaining the near-circularity of the autocorrelation function to avoid analysing biased spectra containing strong anomaly trends; and (4) avoid determining the slopes from the exponential, low wavenumber part of the spectra in the cases of layered magnetization. We also describe the details of the new spectral peak forward modelling method and discuss the conditions under which the method can lead to useful results. We found that, despite all these precautions, in some cases, the results can still be erroneous and, therefore, we recommend a critical evaluation of the results by modelling heat flow and taking into account seismic information on the crustal and lithospheric thicknesses and seismic velocities wherever possible. In the southcentral US, east of the Rockies, where the surface heat flow ranges between 40 and 65 mW m^{-2}, we obtained the magnetic bottom depth of 40 $\pm$ 10 km using the approach of the forward modelling of the spectral peak. This range is similar to the seismically derived crustal thickness of 45–50 km, suggesting, therefore, that the entire crust may be magnetic in this region. Because of the uncertainties in the various heat flow contributing parameters, such as the variations in thermal conductivity, radiogenic heat and hydraulic regime, we could not constrain the lithospheric thickness beyond an estimate ranging approximately from 100 to 200 km.

Key words: crust, geothermal evaluation, lithosphere, magnetic anomalies, Southcentral US, spectral analysis.

INTRODUCTION

Deriving the depths to the bottom of magnetic sources in the lithosphere (in many cases identified with the Curie point of magnetic minerals) is important for constraining temperatures in the crust and thus the rheological nature of the Earth's lithosphere. In the last four decades, several methods and their variations have been proposed for estimating this depth from azimuthally averaged Fourier spectra of magnetic anomalies (e.g. Spector & Grant 1970; Bhattacharyya & Leu 1975, 1977; Shuey *et al.* 1977; Connard *et al.* 1983; Okubo *et al.* 1985; Blakely 1988; Pilkington & Todoeschuck 1993; Maus & Dimri 1995; Tanaka *et al.* 1999; Chiozzi *et al.* 2005). In this study, we evaluate the performance of several different methods using model studies on areally large, centrally upwarped, layered and random magnetic models. We also describe the details of the spectral peak of forward modelling method proposed simultaneously by Ravat (2004), Finn & Ravat (2004) and Ross *et al.* (2004) and discuss conditions under which the method can lead to useful results. Furthermore, we investigate the feasibility of forward modelling the power-law expressions (e.g. Maus & Dimri 1995) for the depths of deepest layers from azimuthally averaged magnetic spectra. Even though some of the routinely used methods appeared to work within a tolerable error (a few km), no single technique worked on our model studies with complete reliability and at times produced completely erroneous depths to top and bottom.

More exhaustive model studies showing additional and more complex examples, especially using fractal source models, are possible, but they would not change the conclusion that all depth

Table 1. The factors for converting the spectral slopes to depths using the relationship, slope = factor* Z. Observe the two different definitions of wavenumber. The usage of the term 'wavenumber' without specifying the units has led to confusion in the literature in terms of determining the depths. In this paper, we use the terms frequency (1 km^{-1}) and wavenumber (2π km^{-1}).

Ordinate of the spectral plot	Factor for amplitude spectrum	Factor for power spectrum
Frequency (f) (1 km^{-1})	2π	4π
Wavenumber (1 km^{-1})		
Wavenumber (k) (2π km^{-1})	1	2

estimates must be carefully performed and assessed using tectonic framework, geological and shallow as well as deep geophysical evidence, and heat flow modelling, especially in the cases where high values of heat flow are inferred based on magnetic bottoms lying within the upper and middle crust. In addition, we found that the depth determination methods have been incorrectly used in several published studies and labelled in a way that has caused confusion regarding the usage of the method. Therefore, we also summarize the caveats and usage in this paper.

THE BACKGROUND OF THE METHODS, THE RATIONALE, AND THE KEY OBSERVATIONS

Two types of methods have been commonly used in the spectral estimation of the depth to the bottom of the magnetic layer: the spectral peak method originally given in a landmark paper by Spector & Grant (1970) and used by Shuey *et al.* (1977), Connard *et al.* (1983) and Blakely (1988) among others, and the centroid method originally presented by Bhattacharyya & Leu (1977) and used with certain caveats and variations by Okubo *et al.* (1985) and Tanaka *et al.* (1999). Both methods need *a priori* estimation of the depth to the top of the same layer. During this study, we found that the spectral peaks in the azimuthally averaged spectra are observed only when sources are randomly magnetized as prescribed by Spector & Grant (1970); with uniform magnetization layers, the spectra have power-law form and no spectral peaks are observed.

Spector & Grant (1970) showed that the slopes of logarithms of azimuthally averaged Fourier spectra of magnetic anomalies from ensemble of simple sources are related to the depth to the top of the ensemble and also the spectra have peak positions on the frequency or wavenumber axis that are related to the thickness of the magnetic source layers (see also Table 1). The Spector & Grant (1970) equation, in the notation after Blakely (1995), is

$$|F(k)|^2 = 4\pi^2 C_m^2 |\theta_m|^2 |\theta_f|^2 M_o^2 \, e^{-2|k|z_t} \left(1 - e^{-|k|(Z_b - Z_t)}\right)^2 S^2(a, b), \quad (1)$$

where F is the Fourier power spectrum, k is wavenumber in cycles km^{-1} or 2π km^{-1}, C_m is a constant related to units, θ_m is a factor related to magnetization direction, θ_f is a factor related to magnetic field direction, M_o is magnetization, Z_t and Z_b are the depths to the top and the bottom of the ensemble of magnetic sources, and $S^2(a, b)$ is the factor related to horizontal dimensions of sources.

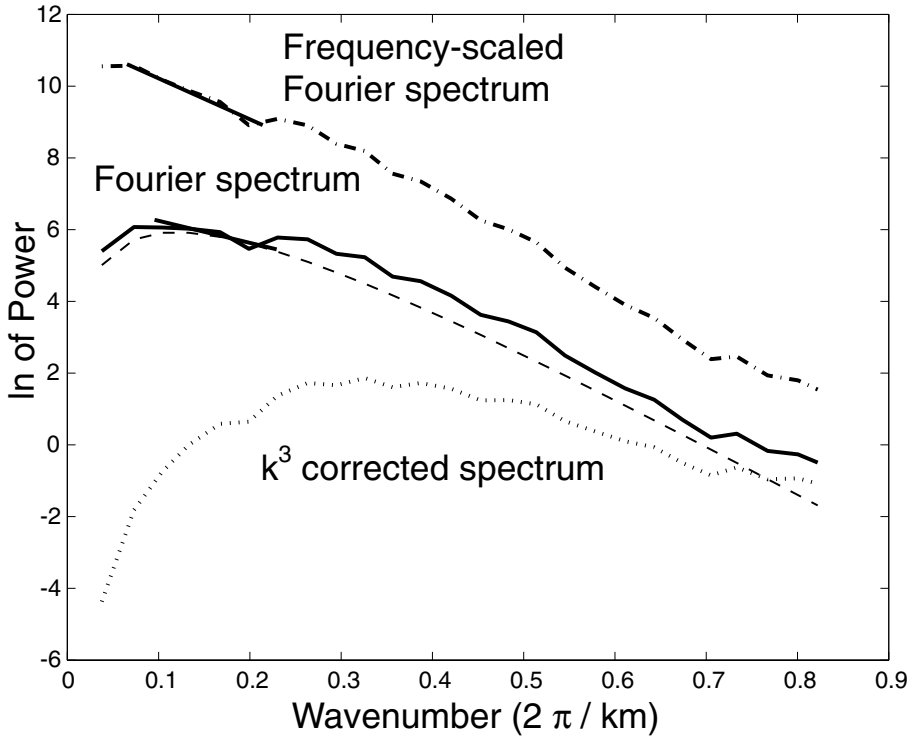

Figure 1. An example of forward modelling of the spectral peak showing the Fourier spectrum (continuous line) and the modelled spectrum (dashed line), and also the frequency-scaled spectrum (heavy dash and dot line) and k^3 corrected spectrum (dotted line) discussed later in the paper. The straight line segments in the k 0.1–0.2 range are linear slope segments for computing depths based on Spector & Grant (1970) and Bhattacharyya & Leu (1977) and Okubo *et al.* (1985) methods. See the text for details. This example is based on the results from 'thin' random source model used later in deriving the depths to deepest layer and will be brought up again in that context. Actual depth to the top is 7.29 ± 1.81 km and bottom is 8.30 ± 2.00 km and depth from Spector and Grant slope is 4.24 km and frequency-scaled spectrum is 6.88 km. k^3 correction overcorrects the spectrum and thus is inappropriate. The continuous dashed line is a result from forward modelling; its depth to the top is ∼6 km and bottom is ∼9 km.

The spectral peak method

The observed spectral peak position (k_{peak}) is a function of Z_t and Z_b and is given by the following transcendental equation (Connard *et al.* 1983; Blakely 1995) from which Z_b can be obtained by trial and error:

$$k_{\text{peak}} = \frac{\ln z_b - \ln z_t}{z_b - z_t}. \quad (2)$$

The limitation of the method is that the spectral peak is not always observed (e.g. spectra of uniformly magnetized layer keeps rising at low wavenumbers with a power-law form (see Blakely 1995), or, trivially, for insufficiently large data windows). Also, many times the peak is represented by a single point and may be uncertain in terms of its position on the abscissa because of either small size windows or the difficulty of deriving precise estimates of power spectrum at the low wavenumbers. To avoid the latter difficulty, careful windowing or multitapering must be performed. Unfortunately, many of the published studies have not been sufficiently careful in taking this precaution and, therefore, the low wavenumber portions of the spectra can have either false peaks or incorrect spectral estimates which could lead to inaccurate depths.

Forward modelling of the spectral peak

Recently, Ravat (2004), Finn & Ravat (2004) and Ross *et al.* (2004) simultaneously proposed forward modelling (iterative matching) of the spectral peak to better estimate the bottom depth by using the part of the eq. (1) that depends on the top and the bottom depths,

$$|F(k)|^2 = C\,(e^{-|k|Z_t} - e^{-|k|Z_b})^2. \quad (3)$$

Here, the constant C, which consists of non-depth-dependent terms in eq. (1), can be adjusted to move the modelled curve up or down to fit the observed peak. The depth to the top of the layer is adjusted also to match the slope adjacent to the spectral peak. Fig. 1 shows an example of the forward modelling procedure that is based on one of the model study results we use later. At this juncture, we are only concerned with the continuous solid line (labelled as the Fourier spectrum) and the dashed line (which is the modelled spectrum generated using an assumed Z_t and Z_b in eq. 3). The assumed Z_b controls the location of the spectral peak (near $k \sim 0.1$ in Fig. 1) and Z_t controls the slope in the high wavenumber range ($k > 0.5$). The slope immediately adjacent to the peak is controlled by the combination of both Z_t and Z_b. For example, deepening the Z_b leads to raising the peak relative to the rest of the modelled curve, and vice versa, and consequently affects the low wavenumber slope on the right side of the peak. Deepening the Z_b also shifts the modelled peak to the left relative to the rest of the curve and also broadens the peak, whereas shallowing the depth to bottom moves the peak to the right and makes them sharper.

The advantage of forward modelling is that it allows one to fit iteratively the position and the width of the peak and match the adjacent part of the slope more precisely and explore the model space

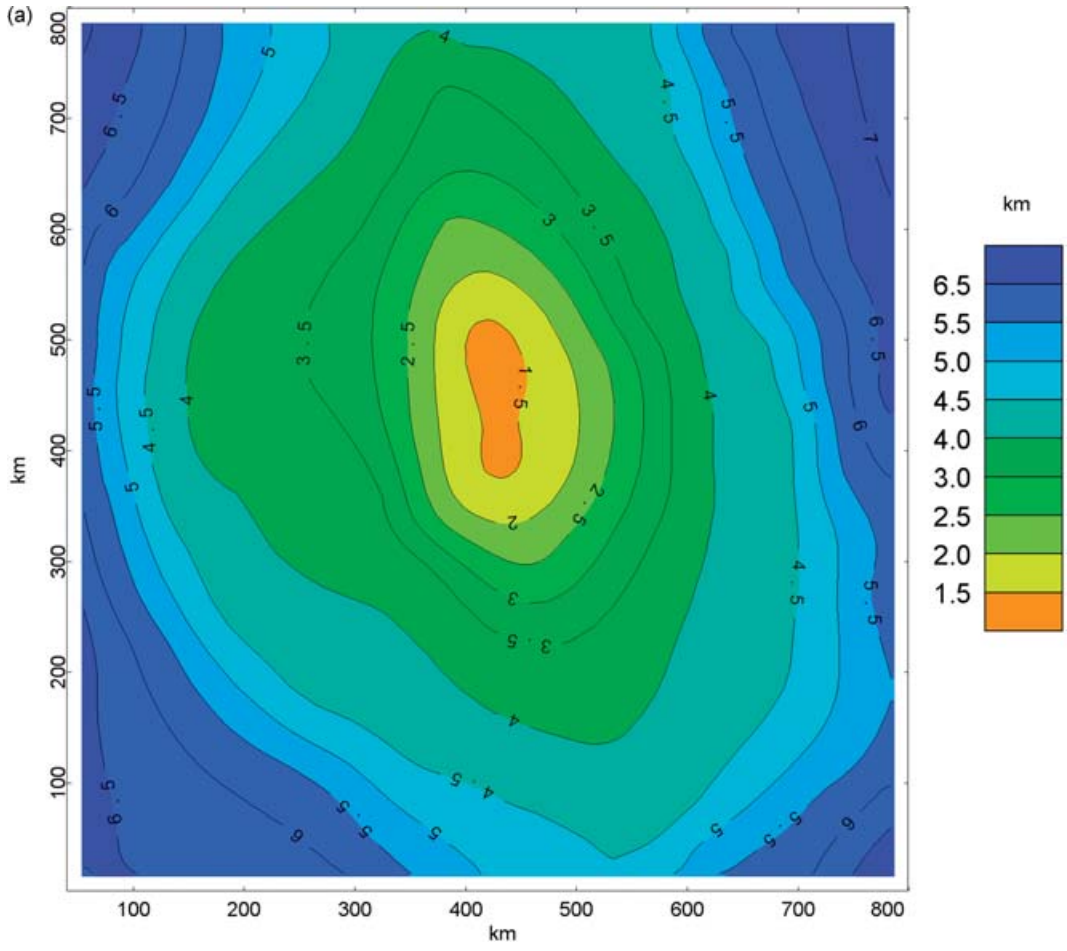

Figure 2. (a) The top of the 'thin' layered source model used in the study and (b) the bottom of the 'thin' layered source model used in the study.

(rather than relying on a single estimate of the abscissa position of the peak which can be unreliable due to having too few spectral samples covering the peak from smaller than adequate size windows). Based on the fit of modelled spectra with the observed, one can accept or reject the results more confidently in this overall subjective process of fitting specific parts of the spectra.

The centroid method

In 1977, Bhattacharyya and Leu published a method for determination of the centroid of rectangular parallelepiped sources, which they had used earlier (Bhattacharyya & Leu 1975) in their study of Curie depths of Yellowstone caldera. In this method, used also by Okubo *et al.* (1985), the estimate of the depth to the centroid (Z_o) is obtained from the slope of an azimuthally averaged frequency-scaled Fourier spectra in the low wavenumber region [$G(k) = 1/fF(k)$, where f is frequency (in 1 km^{-1})] and the estimate of the depth to the top of the source is obtained from the slope of azimuthally averaged Fourier spectrum. Fig. 1 shows the examples of selecting the slopes from the low wavenumber range parts of the Fourier and the frequency-scaled spectra. The depth to the magnetic bottom is then obtained from $Z_b = 2\,Z_o - Z_t$.

Okubo *et al.* (1985), elaborating on the application of the Bhattacharyya & Leu (1977) method, suggested that one could obtain centroid estimates from the high-pass filtered (as low as 40–50 km high-pass) magnetic data; however, this leads to elimination of meaningful part of the spectra related to the depths to the deepest layers of interest. There appears to be a recent consensus among the researchers in the field (Hansen, private communication, 2004; Chiozzi *et al.* 2005; and the results of this study) that the dimension of the window analysed may need to be, in some cases, up to 10 times the depth to the bottom. Many times, it is not practical to analyse windows greater than about 200–300 km because disparate tectonic regimes can be 'averaged' within a single window, diluting the meaningfulness of the results.

In obtaining the depth to the top of the source using this method, Tanaka *et al.* (1999) advocated fitting the slope to a higher wavenumber part of the spectrum than the lowest wavenumber straight slope segment (as shown in Fig. 1), arguing that the linearized equation for the depth to the top is valid for wavelengths greater than the thickness of the layer. This leads to deeper magnetic bottom estimates that, at times, appear to be desirable. However, in applications with real data, different slopes of the Fourier spectra imply existence of multiply layered magnetic structures. Therefore, the major practical limitation in this usage is that the slope from the high-wavenumber part of the spectrum can give the depth to the top of a shallower layer—not the same layer as in the determination of the centroid—and, consequently, give incorrectly a deeper estimate of the bottom of the deeper layer.

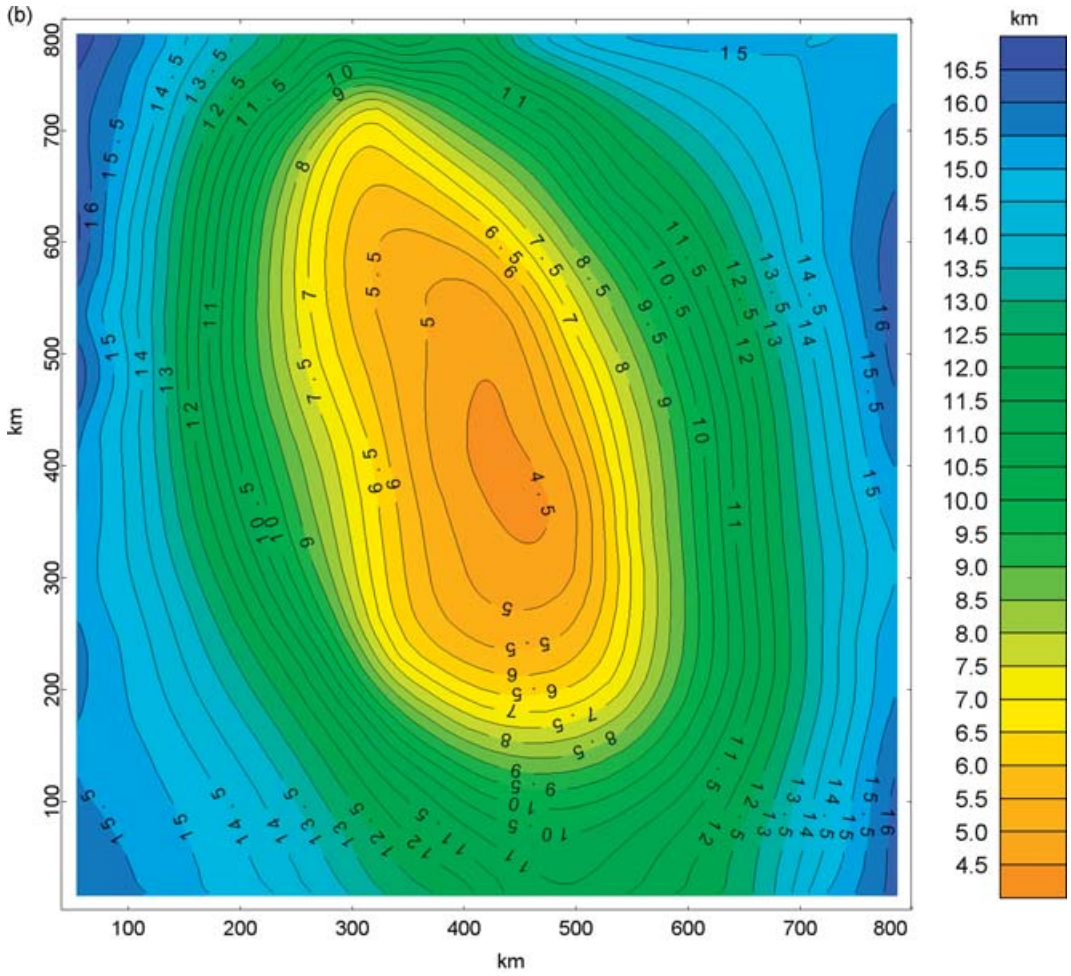

Figure 2. (*Continued.*)

Power-law corrections

Recently, important caveats regarding the depth determination methods have been recognized but have not been considered by many recent users interested in the problem of determination of the magnetic bottom depth, perhaps because not enough time has passed to digest the results. Fedi *et al.* (1997) noted that when the random source variation is large, the Spector & Grant (1970) equation has an inherent power-law form,

$$|F(k)|^2 \propto k^{-2.9}. \quad (4)$$

A similar $k^{-\beta}$ dependence has also been observed for fractal source distributions (e.g. Pilkington & Todoeschuck 1993; Maus & Dimri 1995). For such cases, the spectra can be pre-multiplied with the factor k^{β} prior to computation of depths (Pilkington *et al.* 1994; Fedi *et al.* 1997). We examine the effect of the power-law correction for the layered and uniform random sources, but not fractal source distributions. The power- law correction straightens and flattens fictitious slopes changes in the usual Fourier power spectra of magnetic anomalies and leads to shallower depth estimates (see examples in the above studies). Because both the depth to the bottom estimators mentioned earlier rely on the *a priori* estimates of the depth to the top, the power-law correction is important for the determination of the depth to the bottom.

In this study, we found that when the correction is grossly inappropriate, it overcorrects the spectra such that low wavenumber portion of the spectrum turns over (or dips down toward the low wavenumber end of the axis) (compare the k^3 corrected and Fourier spectra in Fig. 1). An example of appropriate amount of correction is given later. In employing the correction factor, it is possible to explore a strategy of reducing the β factor to yield an appropriate correction for the given situation, but this is cumbersome and we have not attempted it.

It is interesting to note that the approach of Tanaka *et al.* (1999), in which the depth to top is picked from the slope of the adjacent less steep portion of the spectrum compared to the centroid depth, partly achieves the effect of the above power-law corrected flattening. Thus, for single layered model studies, the Tanaka *et al.* approach might be perfectly fine, but as discussed earlier, with their approach in multiple-layer cases, one would most certainly end up picking the depth to the top of the shallower layer which would result in a deeper bottom estimate based on $Z_b = 2\,Z_o - Z_t$.

Since the spectra of layered sources do not produce spectral peaks but have a power law increase in the low wavenumber region, it should be possible to implement forward modelling to estimate the parameters of the deepest layer in this case; an inversion through linear programming for the power-law situation for the top of the magnetic basement has been accomplished by Maus & Dimri (1995). However, the inversion requires that the range of wavenumbers over which the spectra are modelled be pre-selected and be correct; this range, for the deepest layer, is different for different windows and, therefore, difficult to employ in a moving window fashion.

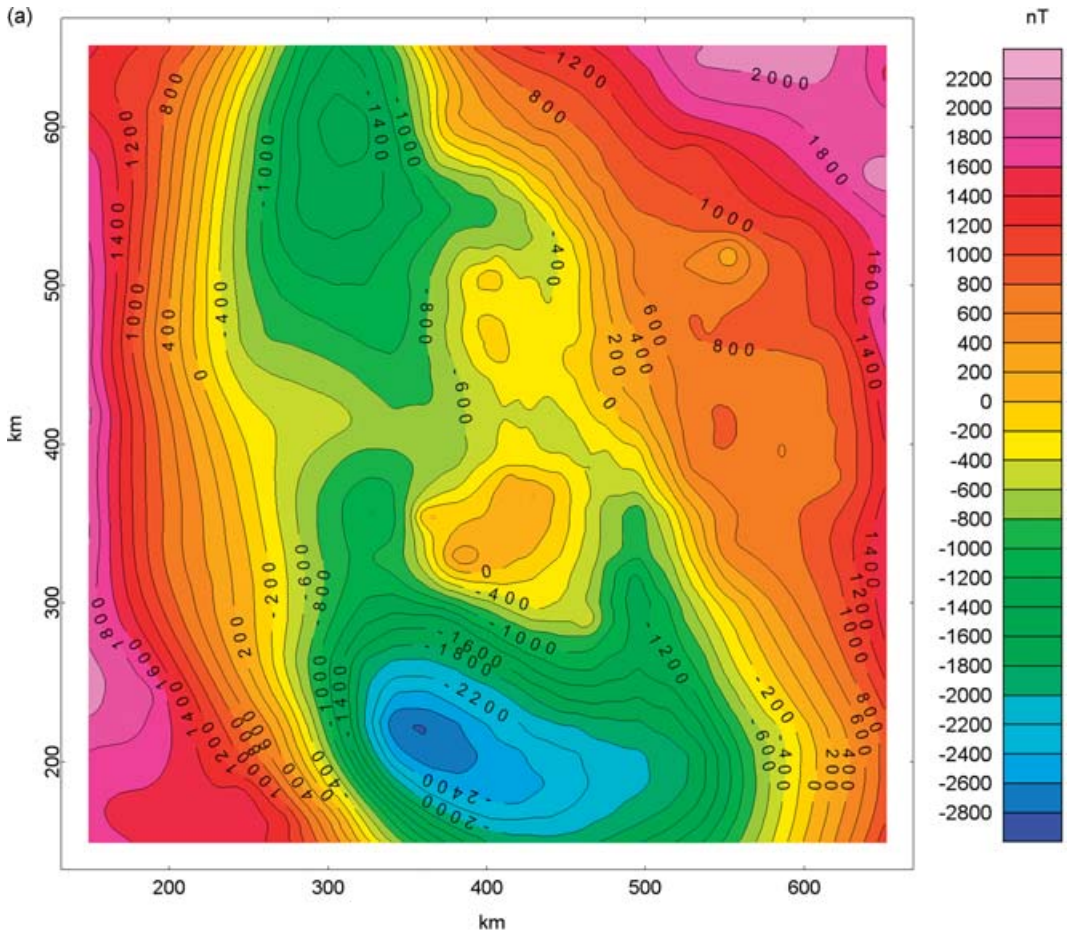

Figure 3. (a) The magnetic field from the 'thin' layered model shown in Fig. 2 and (b) the magnetic field from the 'thin' random source model contained within the source layer shown in Fig. 2. See text for details.

Therefore, we attempted estimating the top and the centroid of the deepest layer by forward modelling and visual comparison of the Fourier spectra in the low wavenumber range to derive the depth to the top and the frequency-corrected spectra to derive the depth to the centroid of the layer. The power-law form of the spectra (Maus & Dimri 1995) is

$$\ln |F(k)|^2 = C - 2Zk - \beta \ln k, \quad (5)$$

where the constant C can be adjusted to move the modelled curve up or down to fit the observed, Z is the depth to the top or the centroid depending upon whether the Fourier or the frequency-scaled spectra are modelled, k is the wavenumber (2π km^{-1}), β is the power-law exponent. In visually trying to fit this equation, we found that there is significant interdependence between all the unknowns (C, Z and β), and it was very difficult to obtain reliable answers letting all parameters vary. The parameters were difficult to derive also in the case where we fixed the value of β to 2 (its most probable value inferred from the study of Maus & Dimri (1995). Thus, for this study, we abandoned the approach of modelling the power-law form and used the approach of modelling the spectral peak to estimate the depth to the top and a 'minimum' estimate on the depth to the bottom as discussed later.

THE MODEL STUDY

We generated magnetic source models of approximately 800 × 800 km dimensions using 2 × 2 km rectangular prisms arranged as either upwarped magnetic layer of constant magnetic properties (7 A m^{-1} induced magnetization), or sources with (uniformly) randomly varying tops and bottoms lying within the upwarped layer geometry with uniformly randomly varying magnetization between ±2 A m^{-1}. The tops and bottoms of one of the layered models are shown in Figs 2(a) and (b), respectively, and the magnetic field at 1 km height above the crust in the field inclination of 60° and declination of 0° produced using the layered and random sources are shown in Figs 3(a) and (b), respectively. We have named these models 'thin' (thickness <10 km with depth to the bottom ranging from 4 to 17 km). We then performed variations on this theme: that is, increased the observation height (equivalent to deepening the layer) and, separately, deepened the bottom of the layer by 10 and 30 km (with designations 'intermediate' and 'thick', respectively). Because the random source models were restricted to lie within the layered sources, deepening the depth of the bottom layer by 30 km still resulted in the average depth to the bottom much lower and the depths to top much deeper than their layered model counterparts and, consequently, the models were actually thin. Such models were classified as 'deep' instead of 'thick' (although their layered counterparts are thick). Lastly, we evaluated the depths to the top and bottom using different window sizes as well as several different methodologies: the depth to the top of the deepest observable layer picked from the slope of the Fourier spectrum (Spector & Grant 1970), performing the k^3 correction of the spectra prior to the computation (Fedi *et al.* 1997), using Tanaka *et al.*'s (1999) approach of using the neighbouring high-wavenumber part of the

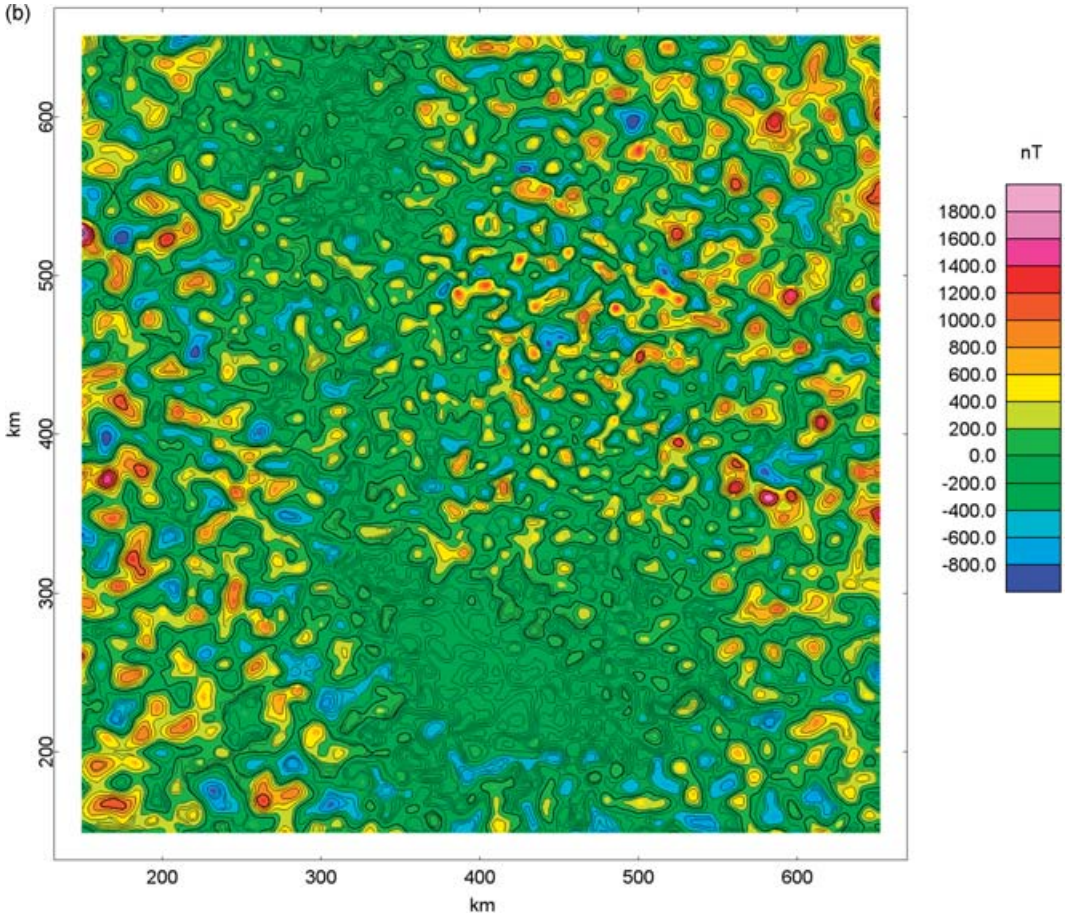

Figure 3. (*Continued.*)

Table 2. The actual depths and depth errors of thin layered source model observed from different heights. Positive depth error is deeper and vice versa. The best estimates are given in bold. Underscore is used to draw attention to the results with large standard deviation of the depth errors.

Source type, observation height	Window size (km)/ number of windows averaged/ comment regarding spectral peaks	Averages and standard deviations of top and bottom depths of all windows (km)	Error in depth to top using slope of Fourier spectra	Error in depth to top using slope of k^3 corrected spectra	Error in depths to top and bottom using Tanaka *et al.* (1999) approach	Error in depth to bottom using frequency scaled Fourier spectra	Error in depth to bottom using frequency scaled k^3 corrected spectra	Error in depths to top and bottom using forward modeling of spectral peak
'Thin' layer,	200/16	4.66 ± 0.62	5.01 ± 2.05	4.73 ± 1.88		–	–	$\mathbf{1.15 \pm 1.15}$
1 km	No peak	7.36 ± 1.71	–	–		$\mathbf{1.16 \pm 1.56}^c$	$\mathbf{0.84 \pm 1.44}^c$	0.89 ± 1.36^a
'Thin' random,	160/24	6.05 ± 1.29	-2.83 ± 0.59	Overcorrected		–	-	$\mathbf{-1.57 \pm 0.44}$
1 km	No clear peak	6.72 ± 1.36	–	–		$\mathbf{-1.27 \pm 0.95}$	Overcorrected	-0.32 ± 0.71^a
'Thin' layer,	300/4	4.62 ± 0.81	4.12 ± 2.80	$\mathbf{-1.33 \pm 1.60}$		–	–	$\mathbf{0.12 \pm 0.82}$
6 km	No peak	7.19 ± 2.15	–	–		4.54 ± 1.81	$\mathbf{0.00 \pm 1.17}$	0.57 ± 0.75^a
'Thin' layer,	300/4	4.62 ± 0.81	$\mathbf{0.70 \pm 1.33}$	-5.61 ± 0.96		–	–	$\mathbf{0.12 \pm 0.31}$
11 km	No peak	7.19 ± 2.15	–	–		$3.09 \pm \underline{7.61}$	$-2.92 \pm \underline{6.38}$	-0.94 ± 1.0^a
'Intermediate'	300/4	4.62 ± 0.81	12.92 ± 3.46	$\mathbf{3.57 \pm 3.06}$	$\mathbf{3.08 \pm 1.12}$	–	–	$\mathbf{-0.88 \pm 2.49}$
layer, 1 km	No peak	17.19 ± 2.15	–	–	$13.73 \pm \underline{8.69}$	8.13 ± 3.56	$\mathbf{-0.43 \pm 2.26}$	-0.16 ± 1.64^a
'Intermediate'	300/4	5.91 ± 1.68	$\mathbf{-1.48 \pm 0.39}$	Overcorrected	$\mathbf{-1.63 \pm 0.42}$	–	–	$\mathbf{-1.41 \pm 0.62}$
random, 1 km	Peak	16.55 ± 1.91	–	–	$0.09 \pm \underline{6.73}$	$4.12 \pm \underline{9.37}$	Overcorrected	$0.20 \pm \underline{5.27}^b$
'Thick' layer,	300/4	4.62 ± 0.81	$\mathbf{2.30 \pm 0.55}$	$\mathbf{-1.65 \pm 0.36}$	$\mathbf{2.26 \pm 0.67}$	–	–	$\mathbf{-0.38 \pm 0.60}$
1 km	No peak, Perhaps not deepest layer	37.19 ± 2.15	–	–	$-1.23 \pm \underline{5.88}$	-6.00 ± 2.23	-20.08 ± 1.89	[a]cannot derive
'Deep' random,	300/4	20.80 ± 9.56	-14.16 ± 0.99	Overcorrected	-15.09 ± 0.77	–	–	-13.55 ± 0.81
1 km	Peak, but not deepest layer	28.99 ± 7.45	–	–	-19.05 ± 3.81	-18.10 ± 1.94	Overcorrected	$-2.74 \pm \underline{7.33}^b$
'Thick' layer,	400/1	4.80 ± 0.95	4.35	$\mathbf{-1.47}$	2.69	–	–	$\sim \mathbf{\pm 1}$
1 km	No peak, no slope breaks	37.70 ± 2.71	–	–	6.27	7.81	$\mathbf{-2.36}$	$\sim \mathbf{-5}$ to $\mathbf{-2}$
'Deep' random,	400/1	21.32 ± 9.72	-11.54^d	Overcorrected	-14.21	–	–	$\sim \mathbf{\pm 1}$
1 km	Good peak	29.58 ± 7.70	–	–	$\mathbf{4.17}^c$	-11.01	Overcorrected	$\sim \mathbf{-5}$ to $\mathbf{+5}$
'Deep' random,	500/1	21.56 ± 9.75	$\mathbf{\sim 1}$	Overcorrected	-16.81	–	–	$\mathbf{\sim \pm 1}$
1 km	Good peak	29.86 ± 7.62	–	–	$\mathbf{6.71}^c$	$\underline{6.96}$	Overcorrected	$\sim \mathbf{-5}$ to $\mathbf{+5}$

[a]Minimum estimates because spectral peak not observed.
[b]Estimates with fairly large spread of bottom depth could be obtained.
[c]Since the top layer estimate is grossly wrong, the bottom layer estimate is also meaningless.
[d]This estimate differs from the 500 km window primarily because it is derived from wavenumbers in 0.2–0.3 range, whereas the estimate for the 500 km window is derived from the slope adjacent to the spectral peak.

spectrum, and using the power-law equation as in Maus & Dimri (1995), but for the deepest layer. The depth to the bottom was determined from the position of the spectral peak (when present, eq. 2, Connard *et al.* 1983), the slope of the frequency-scaled version of the Fourier spectrum (Bhattacharyya & Leu 1975; Okubo *et al.* 1985), and determination of both the top and the bottom by forward modelling of the spectral peak (when present, eq. 3, Ravat 2004; Ross *et al.* 2004, and by finding a 'minimum depth' as shown in the examples later when the spectral peaks were not present). We programmed the computer code in Matlab; the code allows iterative picking of slopes using different methods and modelling of the spectral peak. Our spectra have been verified using the results of a number of U.S. Geological Survey codes and commercial products. We use tapering of data windows to characterize better the low wavenumber portion of our spectra which is important for determining the magnetic bottoms. We also compute results only when autocorrelation function of the 2-D Fourier spectrum is near circular, indicating absence of trends in the data that could bias the spectra (Shuey *et al.* 1977). Based on the experimentation of the validity of depth estimates under different situations, we find that these are some of the most important prerequisites for deriving meaningful spectra and extracting depths.

We illustrate below the results for some sample calculations and tabulate them in terms of errors for depths evaluated in this study (Table 2). Because of inherent subjectivity in the usage of these methods, for example, the selection of the part of the wavenumbers to fit or extract slopes, we have verified the results at least twice, and in many cases three times, for the procedural consistency. To understand the significance of these concisely presented results, the table must be studied extremely patiently in every detail along with the following description and the figures.

Fig. 4 shows an illustrative computation of one of the windows for the 'thin' layered model. The part (a) of the figure shows the usual Fourier spectrum and the k^3 corrected spectrum. One can observe that the k^3 corrected spectrum is straightened and flattened in the wavenumber range near 0.2 cycles km^{-1} and, in this case, the correction leads to reasonable estimates of both the depths to top and the bottom [using $1/f$ scaled spectra in part (b)]. In all our layered models the lowest wavenumber part of the spectra were exponentially increasing, and the slopes from the exponential parts

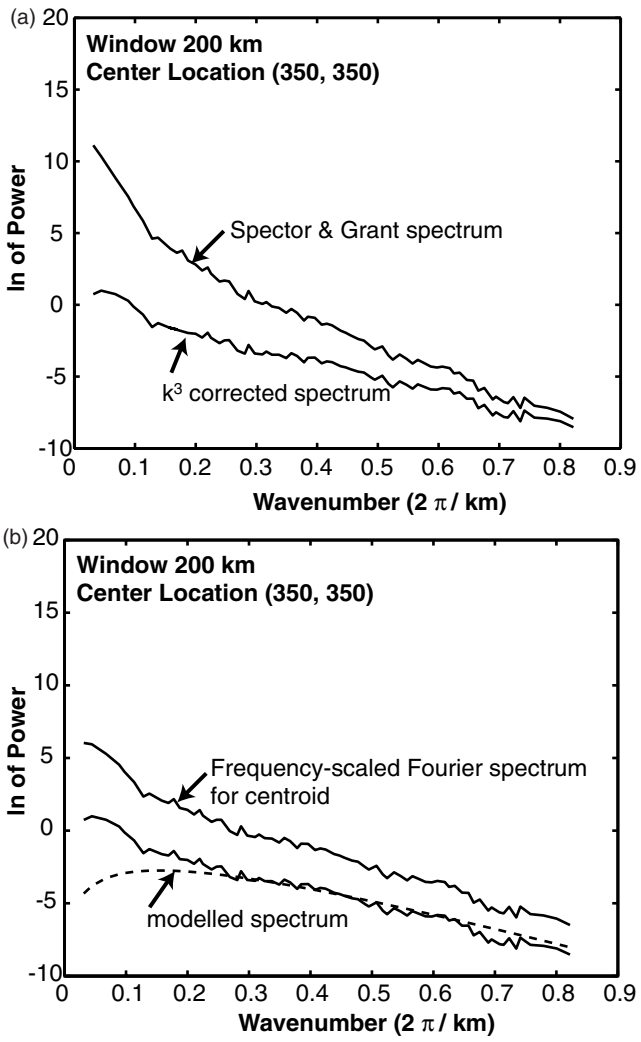

Figure 4. (a) Spectra from 'thin' layer sources used in deriving the depth to the top. Actual depth to the top = 4.52 ± 0.82 and depth from k^3 corrected spectrum = 3.75 km; (b) Illustration of the depth to the bottom estimates. The top curve is $1/f$ spectrum of the k^3 corrected spectrum in part (a). Actual depth to the bottom = 6.23 ± 1.23 and depth from k^3 corrected spectrum = 6.67 km. The continuous curve at the bottom is the k^3 corrected spectrum in part (a) and the dashed line shows the forward modelled spectral peak with the depth to top ∼4–5 km and minimum estimate of the bottom ∼6–7 km.

are not related to depths of layers (slopes from this exponential part has sometimes been used mistakenly in the literature to derive the depths to the deepest layers). From the model, we were able to compute 16 estimates from moving the 200 km window offset by half its width, and the collective results (Table 2, 'thin' layer, 1 km) indicate that the depth to the top could not be derived correctly for most windows from either the Fourier or the k^3 corrected spectra. Also, by virtue of the depth to the bottom depending on the top depth, the results on the bottoms cannot be accepted at their face value. For the 'thin' sources, we did not compute the results of the Tanaka *et al.* (1999) approach; however, those results will be similar to the results of the k^3 corrected spectra because, for single layer cases, the two procedures are effectively similar (as discussed in the previous section).

Since no spectral peak is observed, we determined from the forward modelling approach a 'minimum depth' to the bottom such that the peak would immediately start rolling off the part of the slope being fit without intersecting the observed spectrum (see Fig. 4b). Such a determination cannot be very exact, but appears to work well for many of the examples we tried and could be used to corroborate the results of one of the other techniques if the two estimates were close.

Fig. 1, which we previously used as an example of the spectral peak forward modelling method, shows the results of the uniform random model for a 160 km window. Here, the Fourier spectrum is nearly straight and k^3 corrected spectrum turns over, showing that the latter is overcorrected and inappropriate for depth determinations (also the overturning gives negative, invalid, depths). In this case, results of both the regular Fourier spectrum and the spectral peak forward modelling are reasonable (see the caption of Fig. 1 and Table 2). We show in contour form the derived depth to the top and bottom for this case from the forward modelling approach and the depth error in Figs 5 and 6, respectively. Figs 5 and 6 cannot be directly compared to Fig. 2 because they are computed for the 'random' source model, which lies randomly within the layered model shown in Fig. 2. Also, the 'true' depth estimate in generating the error plot is derived from averaging depths to all of the sources within the observation window as the spectra are similarly averaged. We recognize the limitation that sources outside this window may be contributing to anomalies inside the window; however, there is no perfect method to compute this 'true' quantity and our estimate is a good approximation to the sources that primarily contribute to the observed anomaly. (In order to avoid edge effects, we considered anomalies only between 150 and 650 km locations on both axes. Because the estimate from each window is associated with its central point, there are only a few window locations in the central region from which we could compute the depths.)

Table 2 shows also the results of deepening the 'thin' layer by 5 and 10 km compared to the first model. These results were computed for 300 km wide windows because of the deeper bottom depth. In the first case of 5 km deepening, the k^3 corrected spectra and the forward modelling gave the least error, whereas in the latter case, the slope from the Fourier spectrum more correctly predicted the depth to the top. The large scatter in the bottom estimates is evident through the large standard deviation of the depth errors suggesting that the small average error is meaningless. Once again, the forward modelling gave the best results, albeit with the minimum depth estimation approach.

One problem that can be highlighted at this juncture is that, in real applications, it would be difficult to tell which method is working correctly among all the available approaches. In some instances, we could select an appropriate method based on the nature of the spectra, but sometimes the pre-selection was not possible and led to results that were quite disparate among different methods. The spectra of these scenarios are perfectly common and it would not be possible to identify the erroneous situations from the appearance of the spectra. To avoid erroneous determinations, one could perhaps look for agreement among several approaches as a confirmation of reliability (not counting the agreement between the k^3 corrected spectra and the Tanaka *et al.* (1999) approach because of their effective similarity).

For 'intermediate' layered source models, the k^3 corrected spectra and the spectral peak forward modelling yield the best top and bottom estimates, whereas the bottom from Tanaka *et al.* (1999) approach gave large scatter of results based on the standard deviation of the depth errors (Table 2). For 'intermediate' random source models, all the depths to the top were reasonable and all the depths to bottom were not.

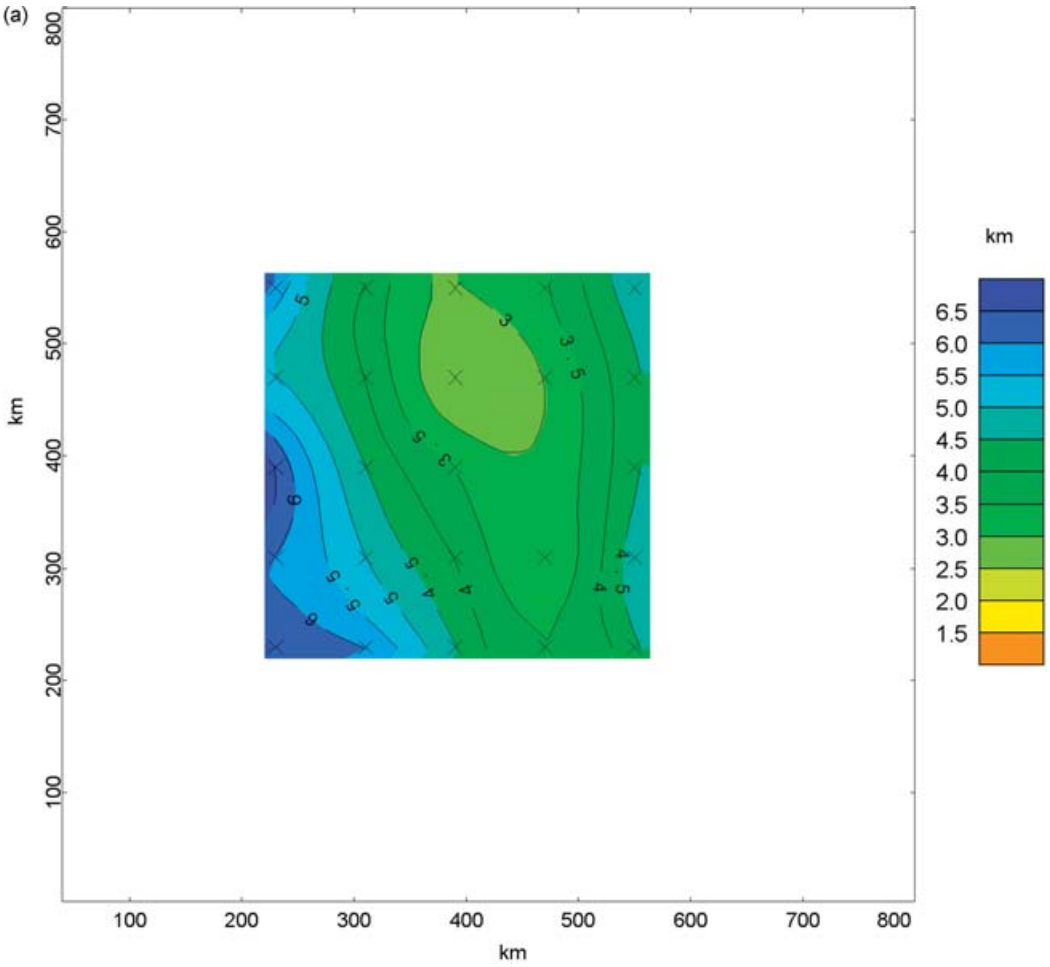

Figure 5. (a) The derived top of the 'thin' random source model from the forward modelling approach; (b) The derived bottom of the 'thin' random source model from the forward modelling approach. Compare with Table 2. Not directly comparable with Fig. 2 because the 'random' source model is contained within the layered model shown in Fig. 2. See text for details.

The 300-km dimension windows were not adequate to analyse the 'thick' layers of this study as seen from the large negative depth errors from all methods (Table 2). This example underscores the importance of computing the spectra and depths with large windows to ensure that the response of the deepest layer is properly captured, and then selecting an adequate window size to allow the maximum spatial resolution.

For 'thick' layered source model with a 400 km window, the k^3 corrected spectra and the spectral peak forward modelling led to good results (a 500 km window was not tried for this), whereas for its random source counterpart, for both 400 and 500 km window sizes, the spectral peak forward modelling gave good results (Fig. 7), and the Tanaka *et al.* approach did not (Table 2). If one picked the slopes from the correct wavenumber range in this case ($\sim$0.075), then the usual Fourier spectrum method gave reasonable results; however, picking slopes from wavenumber range 0.2–0.3 (see Fig. 7) led to erroneous results for the 400 km window case (Table 2). This example illustrates the biggest advantage of the spectral peak forward modelling method: one can exclude incorrect peaks and slope identifications from the spectra by observing the compatibility of the shapes of the observed and modelled peak.

We summarize here our overall procedure. First, we examine the quality of autocorrelation function and classify it subjectively as one of good, fair, or poor so at a later point we can ascribe correctly the confidence one can place in the results. If the autocorrelation function is near circular and the map window does not have anomaly trends, we classify it as 'good'. If there are trends in the anomaly map and the autocorrection function is somewhat oblong then we classify it as 'fair'. Finally, strong trends in the data lead to a significantly trending autocorrelation function, which renders suspect the power spectra computed from azimuthal averaging (that is, the spectra may have segments controlled more by trends in the data than the depth of the layers). We then plot all four spectra (the normal Fourier power spectra as in Spector & Grant 1970; frequency-scaled spectra of Bhattacharyya & Leu 1977; k^3 corrected Fourier spectra of Fedi *et al.* 1977; and frequency-scaled counterpart of the Fedi *et al.* 1997 spectra). Based on whether the latter two spectra turn over or not (see example in Fig. 1), we determine which spectra to fit and which portion of the spectra may represent the deepest layer. If both sets are valid in their appearance, then we make the choice later based on the fit of forward modelling. We then fit least-squares straight slopes to the chosen portion and determine the depths the top and the bottom. Next, we begin forward modelling with the derived estimates to the top and the bottom. Sometimes the forward modelled spectra suggest that the portion we selected to fit with the least-squares approach may not have been a good choice. In such cases, we modify the estimates to achieve the fit to the more

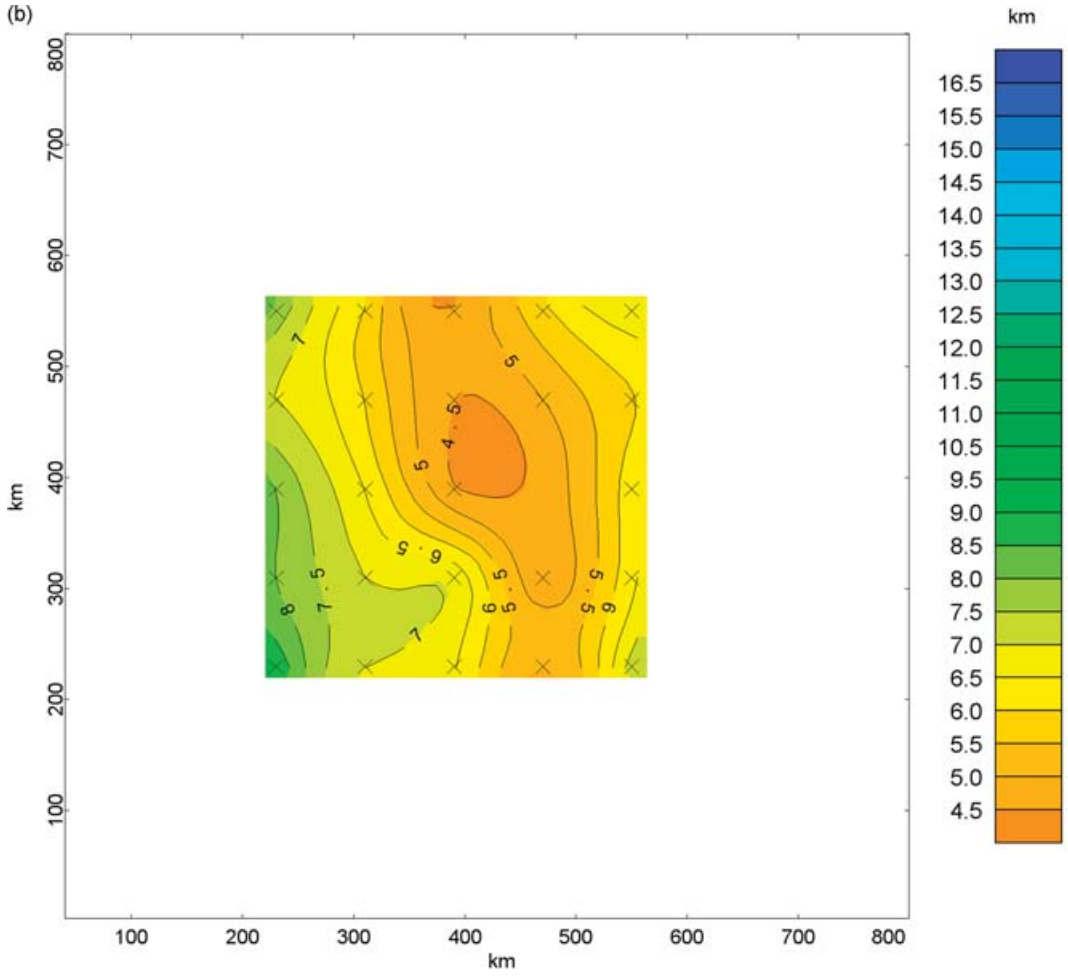

Figure 5. (*Continued.*)

appropriate portion of the spectra on the basis of forward modelling results. When the fit is appropriate, we explore the uncertainty in the depth estimates by examining other acceptable fits. When spectral peaks are not present, we use forward modelling to determine the 'minimum depth' estimate as discussed before. Finally, we do this at 500 to 600 km window sizes to ascertain that we are not missing the spectral peaks by inadvertently choosing a smaller window. Another consideration that is very useful in this process is to try and select windows over geologically/geophysically homogeneous regions and not on the margins of two provinces (Ross *et al.* 2004). We feel that this entire iterative process is important in determining meaningful depth estimates from magnetic anomaly spectra. In addition, it would also be better to seek an external confirmation through other related geophysical results such as the various relevant parameters that contribute to the surface heat flow and seismic determinations of the thickness, and interpretations of tectonic setting in terms of ages and types of rocks at different depths in the crust.

AN EXAMPLE WITH REAL DATA

We extracted magnetic data over a 450 × 350 km region in the southcentral United States (35°N–39°N, 98°W–104°W) from a previously processed National Uranium Reconnaissance and Evaluation magnetic surveys (NURE) flown in 1970s and processed using comprehensive magnetic field model (CM, Sabaka *et al.* 2002) procedure discussed in Ravat *et al.* (2003). The spherical harmonic degree 13 main field model CM was removed from the data; no other regional field was removed. It has been shown before that spherical harmonic degree 13 represents a better cut-off for separation between the main field and the crustal field (Langel & Hinze 1998) and degree 10 IGRFs prior to the epoch 2000 left behind some portion of the main field in the crustal anomaly. With the distribution of ground magnetic observatories and repeat stations in the last fifty years, construction of higher spherical harmonic degree IGRF models have only been possible when magnetic field satellites have been flying. This restriction does not apply to the CM models because they are continuous and use all types of data when they are available and are able to robustly interpolate in between the satellite epochs utilizing the magnetic observatory coverage and physical constraints on the main and external fields variation (Sabaka *et al.* 2002). With spherical harmonic degree 10 IGRF main field, often a non-crustal residual is left behind and scientists had to use arbitrary long-wavelength filtering to overcome the deficiency of those models. Also, piecewise continuous IGRF main field removal can lead to baselevel type shifts in the neighbouring surveys flown at different times and cause further long-wavelength problems (see Ravat *et al.* 2003) The individual (2° of longitude × 1° of latitude) NURE surveys are flown at the terrain clearance of about 100–140 m at roughly 10 km spacing between the lines, but the surveys can be gridded at 1 km spacing because of closer sampling of about 60 m along the flightlines. Fig. 8 shows the Fourier, the frequency-scaled, and the spectral peak forward modelled power spectra derived from a 320 ×

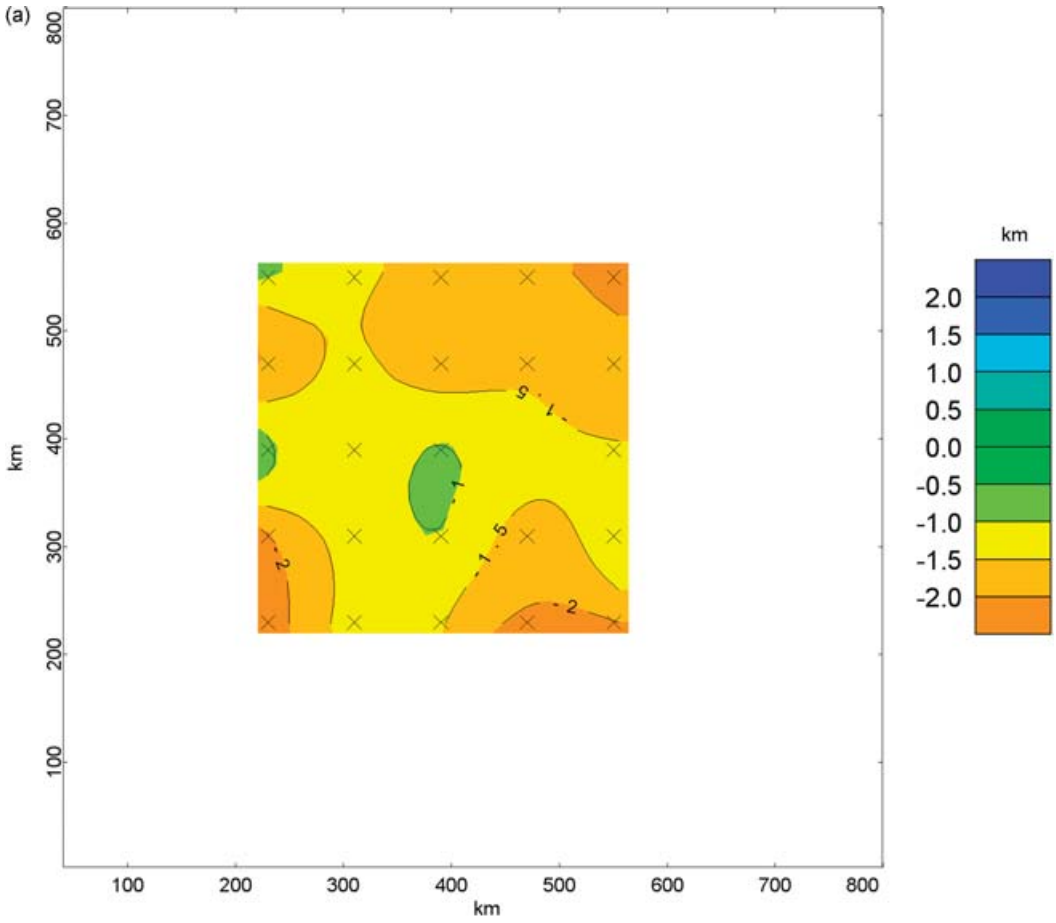

Figure 6. (a) The depth error (derived—true) for the top of the 'thin' random source model from the forward modelling approach; (b) The depth error (derived—true) for the top of the 'thin' random source model from the forward modelling approach. Compare with Table 2. 'True' estimate is computed by averaging depths of all of the sources within the observation window. These results are not directly computable from Fig. 2 and Fig. 5 because of the averaging and also because the 'random' source model is contained within the layered model. See text for details.

320 km window (with a 5 km grid interval). In this study area, these spectra did not differ very much with respect to the spectra from the new North American Magnetic Anomaly database (Bankey *et al.* 2002) because different surveys in this region may have been adjusted well with respect to each other during the compilation of the map (although wavelengths longer than 500 km had to be corrected using CHAMP satellite anomalies). There were no additional peaks when we used the North American magnetic compilation and increased window sizes to 600 km in the same region. This suggests that our 320 km window was adequate to determine the depth to the magnetic bottom.

The forward modelling approach for the spectra in Fig. 8 shows that wide range of magnetic bottom estimates (40 $\pm$ 10 km) are possible for these data and this range is more realistic than choosing single values from the direct estimate using eq. (2) ($\sim$35 km) or the slope of the frequency-scaled spectra ($\sim$44 km) that depend on the subjective selection of the slope segment in deriving depths. Despite the wide range in the estimated bottom range, we would like to suggest that the magnetic depth estimates are useful in placing useful constraints on the temperatures in the lithosphere, especially when taken in the context of availability and uncertainties in the other geophysical models. We show the uncertainties of other data and the contribution of the magnetic bottom depth results below.

Surface heat flow (q_s) in the region of the above example ranges from 40 to 65 mW m^{-2} based on the Geothermal Map of North America published in 2004 by American Association of Petroleum Geologists (AAPG); however, the point data in Global Heat Flow Database (http://www.heatflow.und.edu/index2.html) indicates that the above values are based on interpolation of neighbouring values. Nonetheless, we have examined this range of heat flow values using the steady state 1-D geotherm modelling equations of Lachenbruch & Sass (1978) and assuming that the lithosphere–asthenosphere boundary is governed by dry peridotite solidus with solidus-depth relationship of Tsolidus = 1200 °C + 2.5 °C km^{-1} * Depth (km) (figure 10.6b in Fowler 2005). Assumptions of steady state heat flow and dry peridotite solidus are quite reasonable for this region of the US where the Southern Granite Rhyolite province of *ca*. 1370 Ma dominates the last magmatic episode (Van Schmus *et al.* 1996). The region of our example is more than 500 km away from the lithospheric thinning in the northern Rio Grande Rift and, therefore, we do not anticipate any large 2-D or transient effects. The nearest determination of the lithospheric thickness to our knowledge, which is more than 500 km to SSW, is from the NW–SE trending LA RISTRA experiment described in West *et al.* (2004). In their study of shear wave velocity structure of southwest United States, the authors interpreted the depth of lithosphere–asthenosphere boundary at the depth of $\sim$200 km in the southern Great Plains where surface heat flow values of 40 $\pm$ 10 mW m^{-2} have been measured; however, the thermal conductivity in this region from the U.S. heat flow database is 4–5 Wm^{-1} K^{-1} (which is higher than the

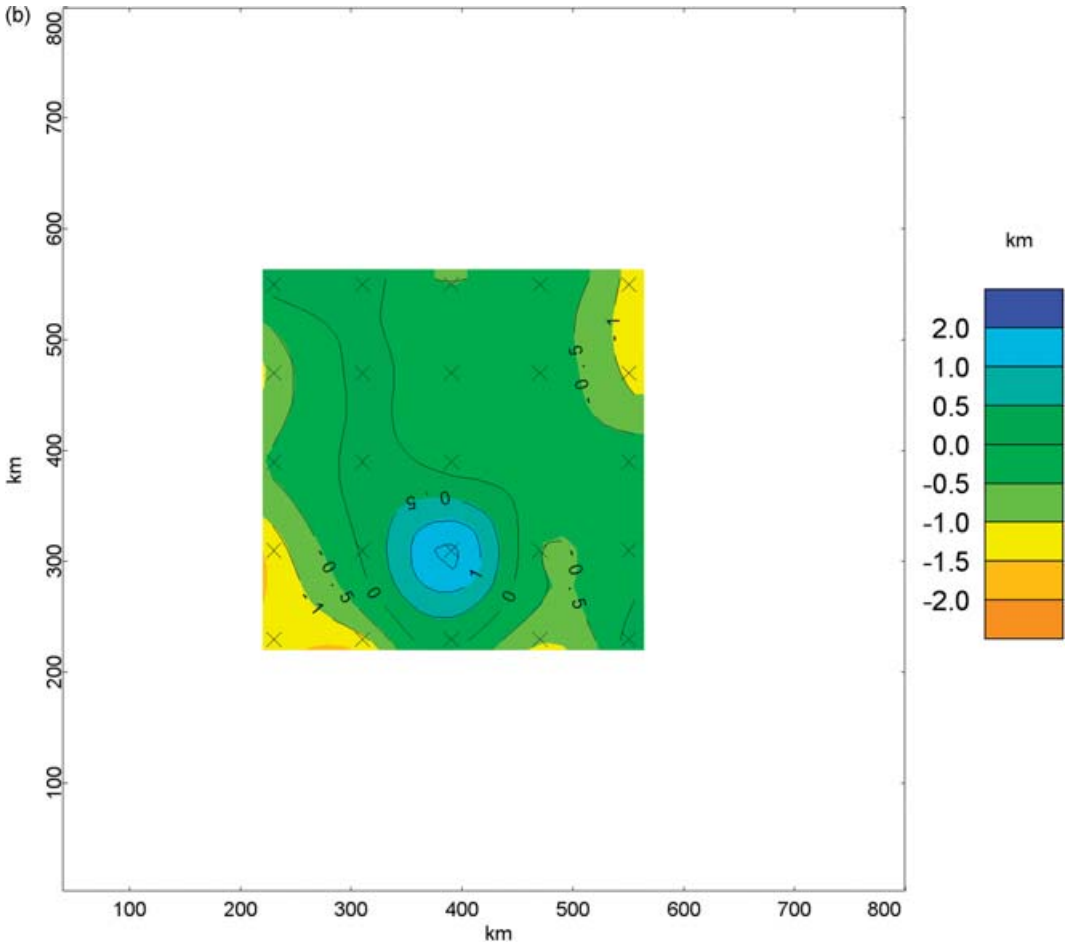

Figure 6. (*Continued.*)

2.5 Wm^{-1} K^{-1} representative average of the region of our example). The interpolated heat flow values across our example range from 40 to 65 mW m^{-2}. It is not clear whether the higher values of heat flow than in the southern Great Plains imply thinner than 200 km lithosphere in our region or this is purely the effect of the thermal conductivity and radiogenic heat production differences between the two regions. For a range of plausible parameters, we have modelled geotherms that produce the surface heat flow range: the asthenospheric heat flow (q_a) on the order 20 mW m^{-2} gives the surface heat flow (q_s) of about 40 mW m^{-2} for the linear heat production of 2.1 μW m^{-3} over a 10 km of radiogenic layer if the lithosphere is 200 km thick (Fig. 9, curves A), or the q_s can be increased to 51–52 mW m^{-2} by increasing the radiogenic heat production by 1.5-fold for the same lithospheric thickness (Fig. 9, curves B). Both these situations lead to the depths of the 580 °C isotherm at 62 and 58 km, respectively, comprising the entire crust and the uppermost upper mantle. The crust in the region is 45–50 km thick (Braile *et al.* 1989) with about 2 km of sedimentary thickness at the top, and the crustal thickness is relevant if the bottom of the magnetic layer is defined by either the Moho or the elevated Curie isotherm within the crust as is widely accepted based on the results of Wasilewski *et al.* (1979) and subsequent studies. Increasing the q_a to 25 mW m^{-2} leads to q_s of 46 mW m^{-2}, reduces the depth of the 580 °C isotherm to ∼50 km, and thins the lithosphere to about 150 km (Fig. 9, curves C), whereas further increasing the q_a to 33 mW m^{-2} (the stable reference example of Lachenbruch & Sass 1978) leads to q_s of 54 mW m^{-2}, reduces the depth of the 580 °C isotherm to ∼38 km, but thins the lithosphere to about 100 km. Without having a direct seismic lithospheric depth estimate, we cannot discriminate among the possibilities presented in Fig. 9. Nonetheless, q_s values of 40–54 mW m^{-2} are consistent with roughly 100–200 km thick lithosphere, the seismic refraction based crustal thickness of 45–50 km and the magnetic bottom depth of 40 ± 10 km as derived from the forward modelling of the spectral peak. In this case, the spread of the bottom depth derived from the magnetic estimate is large and cannot distinguish between thinner or thicker lithosphere situations; however, when such magnetic bottom depths are elevated and have thinned the magnetic portion of the crust, the spectral peaks will be sharper and will help in the selection of geophysical parameters and temperatures within the lithosphere, ultimately helping to constrain better the rheology of the lithosphere. Because of uncertainties in thermal conductivities and radiogenic contribution, in our present example, we can only suggest that the derived magnetic bottoms are reasonable with the available information and give upper and lower bounds on the temperatures within the crust as described above.

CONCLUSION

In this study, we have critically examined the real performance of several spectral magnetic depth determination methods in terms of their capability of determining the depth to the magnetic bottom on random and layered magnetic model sources of different thickness. We find that when the random sources assumption is valid and clear spectral peaks with multiple points are present, then it is possible

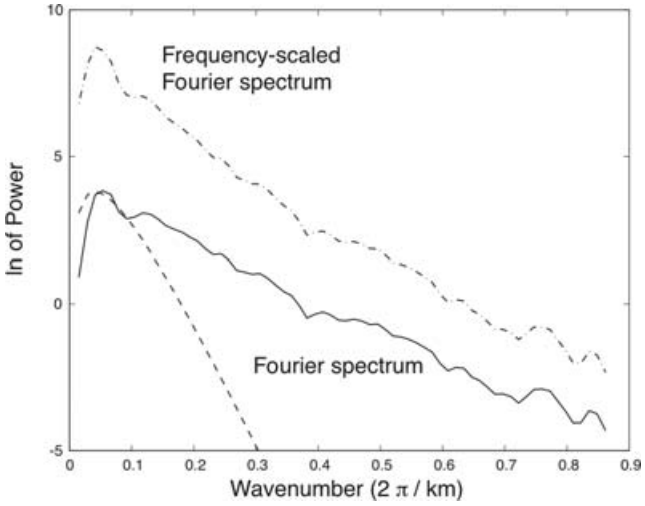

Figure 7. Example of results from 'thick' random source model used in deriving the depth to the top. Actual depth to the top is 21.56 ± 9.75 km and bottom is 29.86 ± 7.62 km and depth from the Fourier spectrum (continuous line) slope is 22.56 km and frequency-scaled spectrum (dash–dotted line) is 36.82 km. The direct use of the spectral peak method (eq. 2) led to the bottom depth of 14–18 km. k^3 correction overcorrects the spectrum (not shown) and thus is inappropriate. The forward modelling (dashed line) leads to depth to the top is ∼22 km and bottom is ∼25 km. The modelled peak cannot be moved significantly to the right by reducing the bottom depth further.

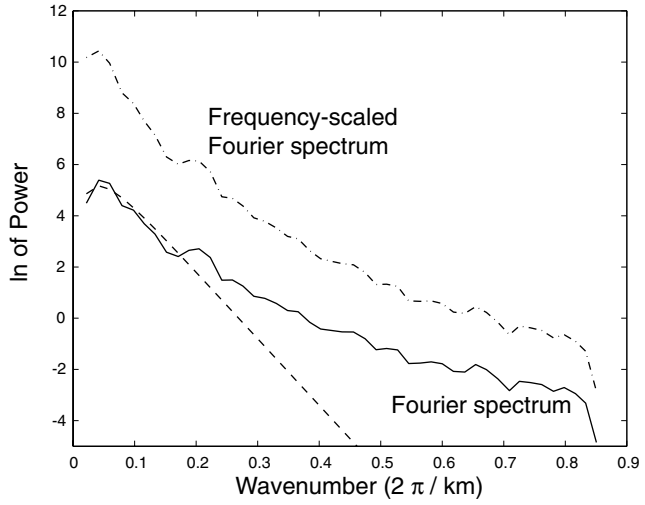

Figure 8. An example with real data. The depth to the top of the deepest layer from Fourier spectrum (continuous line) is ∼12 km and the depth to the bottom from the frequency-scaled Fourier spectrum (dash–dotted line) is ∼44 km. The forward modelling (dashed line) leads to the same depth to the top, and the bottom can be matched at ∼40 ± 10 km. The direct use of the spectral peak method (eq. 2) led to the bottom depth of 35 km.

to determine the depth to bottom more reliably. However, because the spectral peaks are broad for thick magnetic sources, the bottom determination using the spectral peak forward modelling method we have proposed suggests that these determinations can have significantly large uncertainties (10 km or more).

Some of the important considerations in the spectral bottom depth determinations are as follows: (1) having large data windows with widths up to 10 times the expected bottom depth may be required in some cases to ascertain that the response of the deepest layers is captured; (2) compiling magnetic anomalies from modern spherical

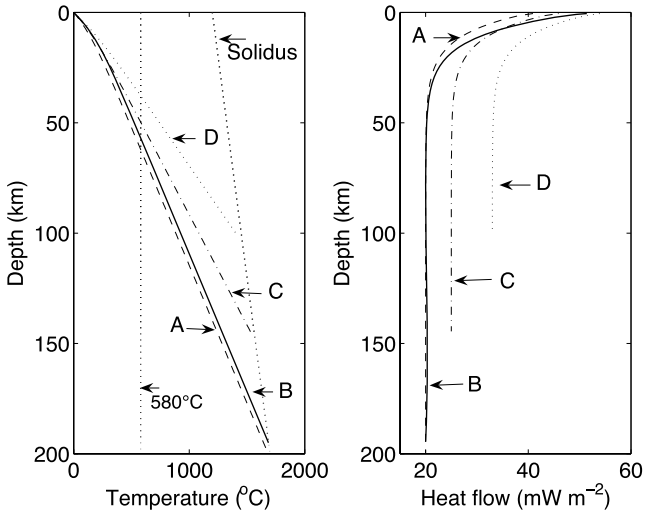

Figure 9. Four possible geotherms from steady state equations of Lachenbruch & Sass (1978) for the real magnetic data set lead to different temperatures in the lithosphere and a range of heat flow between 40 and 54 mW m^{-2}. Two vertical dotted lines on the left panel show 580 °C temperature and the dry peridotite solidus. See the text for details. For all curves the effective depth of heat production is 10 km. Curves (A) asthenospheric heat flow, $q_a = 20$ mW m^{-2}, lithosphere thickness = 200 km, thermal conductivity = 2.5 W m^{-1} K^{-1}, linear heat production, $A_0 = 2.09\,\mu$W m^{-3}, surface heat flow, $q_s = 40$ mW m^{-2}; (B) $q_a = 20$ mW m^{-2}, lithosphere thickness = 195 km, thermal conductivity = 2.5 W m^{-1} K^{-1}, linear heat production, $A_0 = 3.14\,\mu$W m^{-3}, $q_s = 52$ mW m^{-2}; (C) $q_a = 25$ mW m^{-2}, lithosphere thickness = 150 km, thermal conductivity = 2.5 Wm^{-1} K^{-1}, linear heat production, $A_0 = 2.09\,\mu$W m^{-3}, $q_s = 45$ mW m^{-2} and (D) q_a = 33 mW m^{-2} (stable reference geotherm of Lachenbruch & Sass 1978), lithosphere thickness = 95 km, thermal conductivity = 2.5 W m^{-1} K^{-1}, linear heat production, $A_0 = 2.09\,\mu$W m^{-3}, $q_s = 54$ mW m^{-2};

harmonic Earth's main field models (e.g. recent IGRFs or CMs, etc.) for avoiding arbitrary removal of regional fields. Arbitrary regional removal by filtering affects and modifies the low wavenumber part of the spectra and alter the bottom depth estimates; (3) determining the autocorrelation function and determining the depth estimates only for windows where the function is near-circular can ensure that there are no strong trends in the data that modify the slopes of the azimuthally averaged spectra (Shuey *et al.* 1977)—it is better to leave out spectra that are thus modified and lead to erroneous estimates; (4) beginning the determinations with the largest possible windows (>300–500 km windows) to ensure that the response of the deepest layers is captured in the analysis. The window size can subsequently be reduced to improve the spatial resolution if it is permitted by the nature of the spectra; and (5) when the spectra indicate power-law form in the low wavenumber range (and no spectral peak), only minimum bottom depth estimates can be derived using the spectral peak forward modelling procedure. In these cases, it is also important not to fit slopes to the low wavenumber exponential part of the spectra as it would lead to an inaccurate depth determination.

For interpreting the results of the magnetic depth determination in terms of lithospheric temperatures, it is advisable to look for external validation. Modelling of surface heat flow using lithospheric geotherms is important for constraining rheological parameters of the lithosphere but is made difficult by insufficient information on the radiogenic heat generation, thermal conductivity variation of geological units, tectonic and magmatic history of the region and its hydrologic regime. The spectrally derived magnetic bottom estimates can place further constraints for temperatures at certain depths

within the crust for these geotherms when the magnetic depths are above the Moho depth. When the derived depths are close to the Moho depth, based on the Wasilewski *et al.* (1979) inference of the Moho as the magnetic bottom, one may or may not be able to infer the temperatures depending on the thickness of the crust in the region.

ACKNOWLEDGMENTS

We thank Richard Hansen, Richard Blakely, Jeffrey Phillips, Tien Grauch, Gerry Connard, Mark Pilkington, Stefan Maus, Hannah Ross, Ron Sweeney and Carol Finn for substantial input in checking and generalizing our results. We also thank two anonymous reviewers and Editor Cindy Ebinger for comments that improved the manuscript. We are grateful to NASA and Istituto Nazionale di Geofisica e Vulcanologia (INGV) for financial support.

REFERENCES

Bankey, V. *et al.*, 2002, Digital data grids for the magnetic anomaly map of North America, US Geological Survey Open-File Report 02-414 (http://pubs.usgs.gov/of/2002/ofr-02-414/).

Bhattacharyya, B.K. & Leu, L.K., 1975. Analysis of magnetic anomalies over Yellowstone National Park. Mapping the Curie-point isotherm surface for geothermal reconnaissance, *J. geophys. Res.,* **80,** 461–465.

Bhattacharyya, B.K. & Leu, L.K., 1977. Spectral analysis of gravity and magnetic anomalies due to rectangular prismatic bodies, *Geophysics,* **41,** 41–50.

Blakely, R., 1988. Curie temperature isotherm analysis and tectonic implications of aeromagnetic data from Nevada, *J. geophys. Res.,* **93,** 11 817–11 832.

Blakely, R.J., 1995. *Potential theory in gravity and magnetic applications*, Cambridge Univ. Press, Cambridge.

Braile, L.W., Hinze, W.J., von Frese, R.R.B. & Keller, G.R., 1989. Seismic properties of the crust and uppermost mantle of the conterminous United States and adjacent Canada, *Geol. Soc. Am. Memoir,* **172,** 655–680.

Chiozzi, P., Matsushima, J., Okubo, Y., Pasquale, V. & Verdoya, M., 2005. Curie-point depth from spectral analysis of magnetic data in central-southern Europe, *Phys. Earth planet. Int.,* **152,** 267–276.

Connard, G., Couch, R. & Gemperle, M., 1983. Analysis of aeromagnetic measurements from the Cascade Range and in central Oregon, *Geophysics,* **48,** 376–390.

Fedi, M., Quarta, T. & De Santis, A., 1997. Improvements to the Spector and Grant method of source depth estimation using the power law decay of magnetic field power spectra, *Geophysics,* **62,** 1143–1150.

Finn, C.A. & Ravat, D., 2004, Magnetic Depth Estimates and Their Potential for Constraining Crustal Composition and Heat Flow in Antarctica, *EOS, Trans. Am. geophys. Un.,* **85**(47), Fall Meet. Suppl., Abstract T11A-1236.

Fowler, C.M.R., 2005. *The Solid Earth: An Introduction to Global Geophysics*, 2nd edn, Cambridge University Press, Cambridge.

Langel, R.A. & Hinze, W.J., 1998. *The magnetic field of the Earth's lithosphere: the satellite perspective*, Cambridge University Press, Cambridge.

Lachenbruch, A.H. & Sass, J.H., 1978. Models of an extending lithosphere and heat flow in the Basin and Range province, in *Cenozoic tectonics and regional geophysics of the western Cordillera*, pp. 209–250, eds, Smith, R.B. & Eaton, G.P., The Geological Society of America Memoir 152, Geological Society of America, Boulder.

Maus, S. & Dimri, V., 1995. Potential field power spectrum inversion for scaling geology, *J. geophys. Res.,* **100,** 12 605–12 616.

Okubo, Y., Graf, R.J., Hansen, R.O., Ogawa, K. & Tsu, H., 1985. Curie point depths of the island of Kyushu and surrounding areas, Japan, *Geophysics,* **53,** 481–494.

Pilkington, M. & Todoeschuck, J.P., 1993. Fractal magnetization of continental crust, *Geophys. Res. Lett.,* **20,** 627–630.

Pilkington, M., Gregotski, M.E. & Todoeschuck, J.P., 1994. Using fractal crustal magnetization models in magnetic interpretation, *Geophys. Prospect,* **42,** 677–692.

Ravat, D., 2004. Constructing full spectrum potential-field anomalies for enhanced geodynamical analysis through integration of surveys from different platforms (INVITED), *EOS, Trans. Am. geophys. Un.,* **85**(47), Fall Meet. Suppl., Abstract G44A-03.

Ravat, D., Hildenbrand, T.G. & Roest, W., 2003. New way of processing near-surface magnetic data: The utility of the Comprehensive Magnetic Field Model, *The Leading Edge,* **22,** 784–785.

Ross, H.E., Blakely, R.J. & Zoback, M.D., 2004. Testing the Utilization of Aeromagnetic Data for the Determination of Curie-Isotherm Depth, *EOS, Trans. Am. geophys. Un.,* **85**(47), Fall Meet. Suppl., Abstract T31A-1287.

Sabaka, T.J., Olsen, N. & Langel, R.A., 2002. A comprehensive model of the quiet-time, near-Earth magnetic field: phase 3, *Geophys. J. Int.,* **151,** 32–68.

Shuey, R.T., Schellinger, D.K., Tripp, A.C. & Alley, L.B., 1977. Curie determination from aeromagnetic spectra, *Geophys. J. R. astr. Soc.,* **50,** 75–101.

Spector, A. & Grant, F.S., 1970. Statistical models for interpreting aeromagnetic data, *Geophysics,* **35,** 293–302.

Tanaka, A., Okubo, Y. & Matsubayashi, O., 1999. Curie point depth based on spectrum analysis of magnetic anomaly data in East and Southeast Asia, *Tectonophysics,* **306,** 461–470.

Van Schmus, W.R., Bickford, M.E. & Turek, A., 1996. Proterozoic geology of the east-central Midcontinent basement, *Geol. Soc. Am. Special Paper,* **308,** 7–32.

Wasilewski, P.J., Thomas, H.H. & Mayhew, M.A., 1979. The Moho as a magnetic boundary, *Geophys. Res. Lett.,* **6,** 541–544.

West, M., Ni, J., Baldridge, W.S., Wilson, D., Aster, R., Gao, W. & Grand, S., 2004. Crust and upper mantle shear wave structure of the southwest United States: Implications for rifting and support for high elevation, *J. geophys. Res.,* **109,** B03309, doi:10.1029/2003JB002575.